Theor Chem Acc (2009) 124:29–36
DOI 10.1007/s00214-009-0573-5

REGULAR ARTICLE

The effect of phenyl group on the electronic and phosphorescent properties of cyclometalated analogues of platinum(II) terpyridine complexes: a theoretical study

L. L. Shi · T. Li · S. S. Zhao · H. Li · Zhongmin Su

Received: 12 March 2009 / Accepted: 17 April 2009 / Published online: 13 May 2009

Abstract In this work, we theoretically investigate the effect of phenyl group on the electronic and phosphorescent properties of cyclometalated platinum(II) complexes, thereby designing an efficient blue emitting material. Three platinum(II) complexes Pt(N^N^N)Cl (N^N^N = terpyridine), Pt(N^C^N)Cl (N^C^N = 1,3-di(2-pyridyl)-benzene) and Pt(N^N^C)Cl (N^N^C = 6-phenyl-2,2′-bipyridines) are chosen as the models. Their electronic and phosphorescent properties are investigated utilizing quantum theoretical calculations. The results reveal that the phenyl group significantly affects the molecular and electronic structures, charge distribution and phosphorescent properties. The coordination bond length trans to phenyl group is the longest among the same type of bonds owing to the trans influence of phenyl group. Moreover, the phenyl group largely restricts the geometry relaxation of cyclometalated ligand. The strong σ-donor ability of Pt–C bond makes more electrons center at Pt atom and the fragments trans to phenyl group. In comparison with Pt(N^N^N)Cl and Pt(N^N^C)Cl, the complex Pt(N^C^N)Cl has the smallest excited-state geometry relaxation and the biggest emission energy and spatial overlap between the transition orbitals in the emission process. As a result, Pt(N^C^N)Cl has the largest emission efficiency, which well agrees with the experimental observation. Based on these calculation results, a potentially efficient blue-emitting material is designed *via* replacing pyridine groups in Pt(N^C^N)Cl by 3-methylimidazolin-2-ylidene.

Keywords Platinum(II) complexes · Electronic structures · Phosphorescent properties

L. L. Shi · S. S. Zhao · H. Li · Z. Su (✉)
Institute of Functional Material Chemistry,
Faculty of Chemistry, Northeast Normal University,
130024 Changchun, Jilin, China
e-mail: zmsu@nenu.edu.cn

T. Li
State Key Laboratory of Electroanalytical Chemistry,
Changchun Institute of Applied Chemistry,
Chinese Academy of Sciences, 130022 Changchun, Jilin, China

1 Introduction

Luminescent Pt(II) complexes have exhibited tremendous potential in area of optoelectronic applications, especially as triplet dopant emitters in organic light-emitting devices (OLEDs) [1–7]. Due to the unique feature of the coordinative unsaturation, the square planar d^8 systems were allowed to engage in intermolecular interaction including the formation of excimers. If the luminescent spectra of the excimer and monomer span the visible region, single dopant white-light OLEDs can be obtained by using these Pt(II) complexes [1, 8]. Recently, cyclometalated ligands have proved to be beneficial to the luminescence quantum yields for these Pt(II) complexes [9–15]. Williams et al. [16] reported that a class of cyclometalated Pt(N^C^N)Cl (N^C^N = 1,3-di(2-pyridyl)-benzene) complexes have much higher quantum yield (Φ) of 0.6–0.68 in CH_2Cl_2. Subsequently, Yang and his co-workers [8] further designed an efficient blue emitter Pt(II) [1,3-difluoro-4,6-di(2-pyridinyl)benzene] chloride (Pt-4) based on Pt(N^C^N)Cl complex, and its quantum yield reaches to 0.46. These phenomena inspire us to explore the advantages of Pt(II) complexes with N^C^N ligand and the effect of phenyl group on the electronic and spectral properties of these cyclometalated tridentate Pt(II) complexes. In this regard, three models Pt(N^N^N)Cl (N^N^N = terpyridine), Pt(N^C^N)Cl and Pt(N^N^C)Cl

(N^N^C = 6-phenyl-2,2′-bipyridines) were chosen to study the effect of the presence and position of phenyl group on molecular structure, geometry relaxation, electronic structure and phosphorescent properties. Then the theoretical guidance can be obtained for designing efficient luminescent materials and improving the rate of the kinetic substitution reaction.

To the best of our knowledge, there are many efficient green and red phosphorescent materials using Pt(II) complexes, whereas efficient blue-emitting ones are seldom reported [5, 7]. Thus, new efficient blue emitters which can be comparable to the reported complex Pt-4 are required. Herein, we design a cyclometalated Pt(II) complex using *N*-heterocyclic carbene group 3-methylimidazolin-2-ylidene instead of pyridine fragments in Pt(N^C^N)Cl. In view of its high emission energy, small lowest triplet excited-state geometry relaxation and large radiative rate, we presume the designed molecule is an efficient blue phosphorescent emitter.

2 Computation methods

The ground states (S_0) for each molecule were calculated using density functional theory (DFT) [17, 18]. DFT calculations have proved to be remarkably successful in calculating molecular orbital distributions for the interpretation of electrochemical and photochemical results of Ru(II) [19] and square planar Pt(II) complexes [20]. Becke's three-parameter hybrid method [21] using the Lee–Yang–Parr correlation functional [22, 23] (denoted as B3LYP) was adopted here. Subsequently, vibrational frequencies were performed at the same theoretical level to confirm that each conformation was a minimum on the potential energy surface. The geometry optimizations of the lowest triplet states (T_1) were performed by the unrestricted B3LYP method. On the basis of S_0 and T_1 optimization, the TD-DFT approach [24, 25] was applied to investigation of the excited-state electronic properties.

In the calculations, The LANL2DZ and 6-31G(d) basis sets were used for the Pt atom and the other atoms, respectively. Moreover, one f-type polarization function ($\zeta_f = 0.14$) [26] was augmented on the Pt atom to obtain reasonable geometric structures and accurate spectroscopic properties. Zhang et al. have demonstrated that, for both ground and excited states calculations, the validity of using different basis sets for different atoms in the molecules [27]. These computational methods and basis sets have been proved reliable for this kind of cyclometalated Pt(II) complexes [28, 29]. All calculations were performed with Gaussian 03 [30] software package.

3 Results and discussion

3.1 Molecular geometries and feedback bond in ground states

The molecular structures of our investigated complexes are shown in Fig. 1. In all cases, the d^8 metal center adopts a distorted square planar coordination geometry. The Pt(N^N^N)Cl and Pt(N^C^N)Cl possess C_{2v} symmetry, while Pt(N^N^C)Cl is C_s symmetrical. Table 1 lists the selected bond lengths of the three molecules in S_0 and T_1 states, whose experimental data are available. The labels used in Table 1 are shown in Fig. 1. It is found that the calculated results agree well with the experimental values [9, 31, 32], indicating our used calculation methods are reliable. All atoms in our studied complexes are in a plane. This configuration stabilizes the molecular energy due to the extended π-conjugation. The bite angles A_2–Pt–A_3 are nearly 161° for these complexes.

Table 2 summarizes the bond lengths in different electronic environments in S_0 states. For example, the Pt–N bonds trans to Cl are 1.968 and 1.985 Å, and the Pt–N bonds trans to pyridine groups are 2.054 and 2.068 Å; while the Pt–N bond trans to phenyl group is 2.194 Å. It can be seen that the same type of bonds sharing the similar electronic environment are almost of equivalent length. Moreover, the bonds trans to phenyl group are the longest, and the bonds trans to pyridine group are longer than those trans to Cl. It follows that the order of trans influence is phenyl group > pyridine group > Cl. Thus, the presence and position of phenyl group affects the molecular geometries, leading to the different geometry relaxation discussed below.

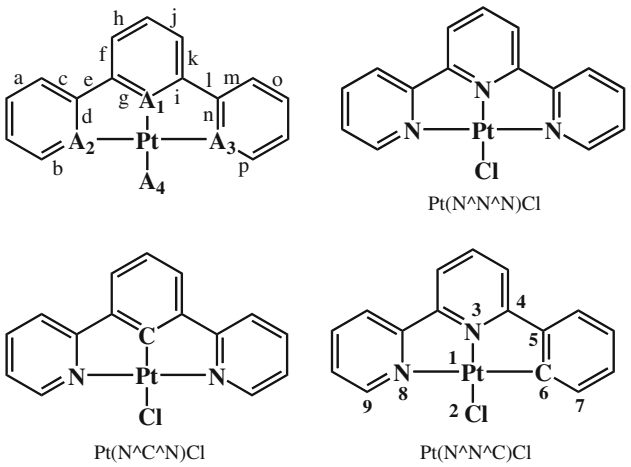

Fig. 1 The schematic structures, atom and bond labels for Pt(N^N^N)Cl, Pt(N^C^N)Cl and Pt(N^N^C)Cl

Table 1 Calculated geometry parameters in S_0 and T_1 states and their difference (Δ_{T1-S0}, in parentheses) for Pt(N^N^N)Cl, Pt(N^C^N)Cl and Pt(N^N^C)Cl with their experimental data (unit: Å)

	Pt(N^N^N)Cl			Pt(N^C^N)Cl			Pt(N^N^C)Cl		
	S_0	Exp. [9]	T_1 (Δ_{T1-S0})	S_0	Exp. [31]	T_1 (Δ_{T1-S0})	S_0	Exp. [32]	T_1 (Δ_{T1-S0})
Pt–A_1	1.968	1.930	1.963 (−0.005)	1.926	1.908	1.899 (−0.027)	1.985	1.943	1.985 (0)
Pt–A_2	2.054	2.025	2.015 (−0.039)	2.068	2.038	2.068 (0)	2.194	2.132	2.131 (−0.063)
Pt–A_3	2.054		2.015 (−0.039)	2.068	2.038	2.068 (0)	1.992	1.995	1.959 (−0.033)
Pt–A_4	2.341	2.307	2.359 (0.018)	2.457	2.417	2.429 (−0.028)	2.353	2.312	2.366 (0.013)
*R*e	1.481	1.472	1.437 (−0.044)	1.470	1.480	1.452 (−0.018)	1.484	1.489	1.420 (−0.064)
*R*l	1.481		1.437 (−0.044)	1.470		1.452 (−0.018)	1.464	1.490	1.464 (−0.001)

Table 2 The bond length for each bond type in S_0 state

Bond type	Bond length (Å)
Pt–C (trans to Cl)	1.926
Pt–C (trans to pyridine group)	1.992
Pt–N (trans to Cl)	1.968, 1.985
Pt–N (trans to pyridine group)	2.054, 2.068
Pt–N (trans to phenyl group)	2.194
Pt–Cl (trans to pyridine group)	2.341, 2.353
Pt–Cl (trans to phenyl group)	2.457

Table 3 Second-perturbation energy $E(2)$ (unit: kcal/mol) of 5*d*-electrons and ligand fragments (L_{A1}, L_{A2} and L_{A3} represent groups A_1, A_2 and A_3, respectively) interaction for Pt(N^N^N)Cl, Pt(N^C^N)Cl and Pt(N^N^C)Cl

System	Donor (*i*) 5d-electrons	Acceptor (*j*) ligand fragments	$E(2)$
Pt(N^N^N)Cl	LP(4)Pt_1	BD*(2) N_3–C_4 (L_{A1})	7.78
	LP(3)Pt_1	BD*(2) N_6–C_7 (L_{A2} and L_{A3})	4.80
	LP(2)Pt_1	RY*(1)Cl_2	0.84
	LP(4)Pt_1	RY*(2)Cl_2	0.94
Pt(N^C^N)Cl	LP(4)Pt_1	BD*(2) C_3–C_4 (L_{A1})	14.67
	LP(3)Pt_1	BD*(2) N_8–C_9 (L_{A2} and L_{A3})	4.91
	LP(2)Pt_1	RY*(1)Cl_2	0.53
	LP(4)Pt_1	RY*(3)Cl_2	0.53
Pt(N^N^C)Cl	LP(4)Pt_1	BD*(2) C_3–N_4 (L_{A1})	7.38
	LP(3)Pt_1	BD*(2) N_8–C_9 (L_{A2})	3.90
	LP(3)Pt_1	BD*(2) C_5–C_6 (L_{A3})	9.44
	LP(2)Pt_1	RY*(1)Cl_2	0.92
	LP(4)Pt_1	RY*(2)Cl_2	0.96

LP, BD* and RY* denote the lone-pair (*n*), formally antibonding orbital (π^*) and Rydberg antibonding orbital (n^*), respectively

Furthermore, we demonstrate that feedback-bond energy is closely relative to the trans influence of the groups. The larger a feedback-bond energy between Pt and a group is, the more the electrons back-donate from a 5*d* orbital into the empty π^*(group) orbital, which makes the coordination bond trans to this group weaker (i.e. the trans influence of this group is larger). Table 3 lists the second-perturbation energy ($E(2)$) of 5*d* orbital electrons and π^*(group) orbitals interaction using natural bond orbital (NBO) analysis. The interaction arises from the charge transfer between them. In other words, the $E(2)$ value represents the feedback-bond energy. For each molecule, the feedback-bond energy follows the order of Pt→ phenyl group > Pt→ pyridine group > Pt→ Cl (such as Pt(N^C^N)Cl, 14.67 > 4.91 > 0.53 kcal/mole), which agrees well with the order of trans influence. Among different molecules, the order is also obeyed for groups sharing the similar electronic environment. For example, the feedback-bond energies are 7.78 and 14.67 kcal/mole for LP(4)Pt_1→ central group L_{A1} of Pt(N^N^N)Cl and Pt(N^C^N)Cl, which indicates that the trans influence of phenyl group is higher than that of pyridine group.

3.2 Geometry relaxation between S_0 and T_1 states

Table 1 also lists the difference between bond lengths of S_0 and T_1 states (Δ_{T1-S0}). The change of coordination bond lengths of Pt(N^C^N)Cl is smaller than that of Pt(N^N^N)Cl and Pt(N^N^C)Cl. For the cyclometalated ligands, the Δ_{T1-S0} of bonds linking inter-ring (*R*e and *R*l) is observed. Table 1 shows that the Δ_{T1-S0} of *R*e and *R*l is very small for the bonds linking the phenyl and pyridine groups (−0.018 and 0 Å), while those are larger for the bonds linking the bipyridine groups (−0.044 and −0.064 Å), especially for *R*e in Pt(N^N^C)Cl. It should be noted that these *R*e and *R*l become shorter from S_0 to T_1 states, except for *R*l in Pt(N^N^C)Cl. Thus, we can anticipate that the LUMOs of these molecules possess bonding character in these regions.

To simply clarify the geometry relaxation on cyclometalated ligands, we employ the concept of the difference between the average length of the "single" and "double" bonds. The degree of bond length alternation (BLA) has been used as a structural parameter in interpreting electronic spectra of many classes of conjugated molecules [33, 34]. Herein, BLA can be defined by the following formula:

Table 4 Calculated bond length modification (unit: Å) in S_0 and T_1 states and their difference (Δr_{e-g}) for these Pt(II) complexes

	Pt(N^N^N)Cl	Pt(N^C^N)Cl	Pt(N^N^C)Cl	Pt-4	**1**
$\Delta r_g(A_1–A_2)$	0.015	0.007	0.018	0.005	−0.002
$\Delta r_g(A_1–A_3)$	0.015	0.007	0.001	0.005	−0.002
$\Delta r_e(A_1–A_2)$	−0.012	0.003	−0.036	0.000	−0.009
$\Delta r_e(A_1–A_3)$	−0.012	0.003	0.014	0.000	−0.009
$\Delta r_{e-g}(A_1–A_2)$	−0.027	−0.004	−0.054	−0.005	−0.007
$\Delta r_{e-g}(A_1–A_3)$	−0.027	−0.004	0.014	−0.005	−0.007

$$\Delta r(A_1 - A_2) = (r_a + r_b + r_e + r_h + r_i)/5 - (r_c + r_d + r_f + r_g)/4$$

$$\Delta r(A_1 - A_3) = (r_j + r_g + r_l + r_o + r_p)/5 - (r_k + r_i + r_m + r_n)/4$$

Table 4 lists the BLA of the optimized structures of our studied complexes in the S_0 and T_1 states (Δr_g and Δr_e) and their difference (Δr_{e-g}). In the ground states, the Δr_g is smaller in phenylpyridine group (0.007 and 0.001 Å) than that in bipyridine ring (0.015 and 0.018 Å). It is indicated that the bond length distributes more averagely on phenylpyridine group. In the lowest triplet states, Δr_e is negative in bipyridine ring (−0.012 and −0.036 Å), resulting in their larger Δr_{e-g} (−0.027 and −0.054 Å). The reduced BLA values from S_0 to T_1 states show that these bipyridine rings undergo obvious transformation from aromatic form to quinoid form, especially for the bipyridine ring in complex Pt(N^N^C)Cl. These results are consistent with the change of *R*e and *R*l. The Δ_{T1-S0} of *R*e of Pt(N^N^C)Cl is largest (−0.064 Å), and its bipyridine ring has the biggest Δr_{e-g} (−0.054 Å) and the most obvious quinoid character. The relatively smaller Δr_{e-g} of phenylpyridine indicates that the phenyl ring has the stronger restriction in geometry relaxation.

The lowest Δr_{e-g} of Pt(N^C^N)Cl leads to the smallest geometry relaxation of cyclometalated ligand N^C^N. Combined with the little variation of coordination bond lengths from S_0 to T_1 states, the Stokes shifts and the nonradiative geometry relaxation of Pt(N^C^N)Cl are the smallest when comparing with the other two complexes. Thus, Pt(N^C^N)Cl is thought to have the largest emission efficiency. Our calculated results further support the experimental observation [14, 16, 35]. The quantum yields of Pt(II) complexes with the type of N^N^C ligands are usually lower than that of Pt(II) complexes with the N^C^N ligand [16, 35].

3.3 Electronic structure

To explore the effect of the presence and position of phenyl group on the electronic structure, we draw a comparison between the components of the highest occupied molecular orbital (HOMO) and the lowest unoccupied molecular orbital (LUMO), energy gap (ΔE), and NBO charge distribution of the three investigated complexes.

Table 5 lists the energies and composition of HOMO and LUMO of these complexes. Contour plots of them are shown in Fig. 2. The HOMO of Pt(N^N^N)Cl is mainly characterized as *d*(Pt) and P_z(Cl), while the presence of the phenyl group makes the π_{phenyl} contribute to the HOMO of Pt(N^C^N)Cl and Pt(N^N^C)Cl. The different position of phenyl group results in the different contribution of P_z(Cl) to the HOMO of Pt(N^C^N)Cl and Pt(N^N^C)Cl. Unlike Pt(N^C^N)Cl, P_z(Cl) has little contribution to the HOMO of Pt(N^N^C)Cl. The LUMOs of the three complexes mainly delocalize on pyridine groups. Due to the different π-extension, the energies of LUMOs follow the order of Pt(N^N^N)Cl < Pt(N^N^C)Cl < Pt(N^C^N)Cl. Just like above anticipation, the LUMOs are bonding in the region of *R*e and *R*l bonds of the three complexes, except for *R*l bond of Pt(N^N^C)Cl.

Table 5 shows that the energies of HOMO and LUMO are largely increased when the phenyl group exists, and the

Table 5 The energies and the compositions (%) of HOMO and LUMO, the energy gap (ΔE) and the excitation energies from S_0 to S_1 for Pt(N^N^N)Cl, Pt(N^C^N)Cl and Pt(N^N^C)Cl (unit: eV)

	HOMO		LUMO		ΔE_g	$S_0 - S_1$
	Energy	Composition	Energy	Composition		
Pt(N^N^N)Cl	−9.43	27.4% *d* + 60.1% P_z(Cl)	−6.14	91.5% $\pi^*_{pyridines}$	3.29	2.77
Pt(N^C^N)Cl	−5.48	30.1% *d* + 36.0% P_z(Cl) + 25.3% π_{ph}	−1.93	98.0% $\pi^*_{pyridines}$	3.55	2.89
Pt(N^N^C)Cl	−5.64	32.8% *d* + 50.3% π_{ph}	−2.49	91.3% $\pi^*_{pyridines}$	3.14	2.38

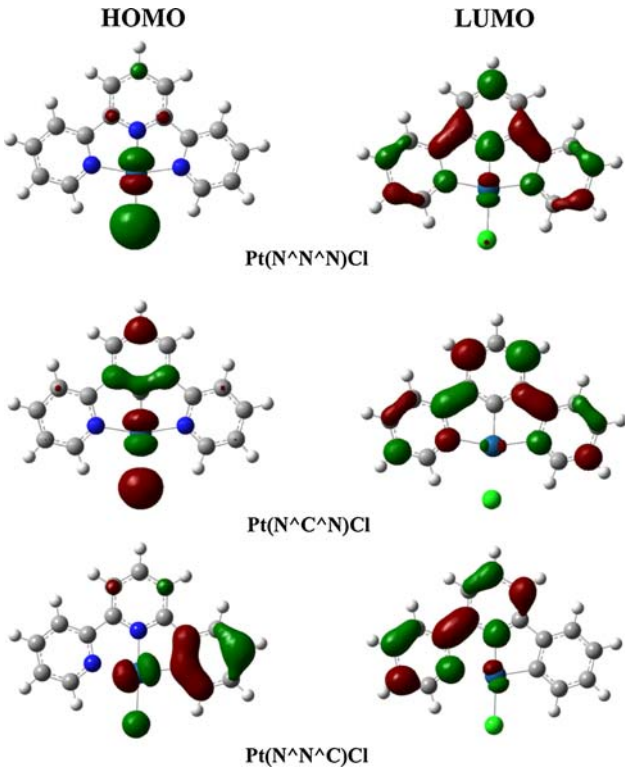

Fig. 2 Contour plots of HOMO and LUMO of Pt(N^N^N)Cl, Pt(N^C^N)Cl and Pt(N^N^C)Cl

ΔE follows the order of Pt(N^C^N)Cl > Pt(N^N^N)Cl > Pt(N^N^C)Cl, which is consistent with the order of the excitation energies from S_0 to S_1. Compared with Pt(N^N^N)Cl and Pt(N^N^C)Cl, the largest ΔE and the smallest geometry relaxation between T_1 and S_0 endow Pt(N^C^N)Cl with the largest triplet energy and shortest emission wavelength (see infra).

The presence and position of phenyl group also influence the charge distribution. The total NBO charges on Pt and each group in the S_0 state are tabulated in Table 6. The strong σ-donor ability of Pt–C bond makes more electrons located at Pt and the fragments trans to phenyl group. For example, the electrons on Cl of Pt(N^C^N)Cl is −0.692, which is more than that of Pt(N^N^N)Cl and Pt(N^N^C)Cl (−0.526 and −0.568, respectively). Hence, the presence and position of phenyl group will influence the rate of the kinetic substitution reaction [32].

Table 6 Total NBO charges on Pt and each group in the S_0 state for Pt(N^N^N)Cl, Pt(N^C^N)Cl and Pt(N^N^C)Cl

	Pt(N^N^N)Cl	Pt(N^C^N)Cl	Pt(N^N^C)Cl
Pt	0.808	0.684	0.652
Ring (A_1)	0.169	−0.306	0.062
Ring (A_2)	0.274	0.157	0.106
Ring (A_3)	0.274	0.157	−0.252
Cl	−0.526	−0.692	−0.568

3.4 The lowest triplet excited states

The TD-DFT method was utilized to calculate the energies of the lowest triplet excited states from the equilibrium geometries of T_1. The calculation results are summarized in Table 7. Meanwhile, a graphical display for the changes of electron density distribution upon $T_1 \rightarrow S_0$ excitation is shown in Fig. 3. From these data it is found that the phenyl group significantly affects the characters of the lowest triplet excited states. The luminescent characters are $d_{Pt}/P_{Cl} \rightarrow \pi^*_{pyridines}$, $d_{Pt}/\pi_{phenyl}/P_{Cl} \rightarrow \pi^*_{pyridines}$ and $d_{Pt}/\pi_{phenyl} \rightarrow \pi^*_{pyridines}$ for Pt(N^N^N)Cl, Pt(N^C^N)Cl and Pt(N^N^C)Cl, respectively. The observed character of Pt(N^C^N)Cl agrees well with the previous calculated results [36]. In TD-DFT calculations, for Pt(N^N^N)Cl and Pt(N^C^N)Cl, the contribution of Cl cannot be neglected, which seems to differ from the experimental investigation. Turki et al. [37] have demonstrated that TD-DFT method overestimates chloride contribution upon electron excitation, with the halide-to-ligand charge transfer being predominant.

It should be pointed out that the direction of $\pi_{phenyl} \rightarrow \pi^*_{pyridines}$ charge transfer of Pt(N^C^N)Cl differs from that of Pt(N^N^C)Cl upon excitation, owing to the different position of phenyl group. This charge transfer is mainly from the phenyl group to the two peripheral pyridine groups and one central pyridine group for Pt(N^C^N)Cl and Pt(N^N^C)Cl, and so the spatial overlap between phenyl and pyridine groups of Pt(N^C^N)Cl is larger than that of Pt(N^N^C)Cl. Consequently, the phosphorescent intensity of Pt(N^C^N)Cl should be stronger than that of Pt(N^N^C)Cl (albeit no oscillator strength of singlet-triplet transition is observed in Table 7, because current TD-DFT method does not consider spin-orbit coupling effects). In a sense, the stronger luminescent intensity of Pt(N^C^N)Cl is another cause for its higher emission efficiency.

The calculated emission wavelength of Pt(N^N^N)Cl, Pt(N^C^N)Cl and Pt(N^N^C)Cl is 598, 533 and 738 nm, respectively (see Table 7). Compared with Pt(N^N^N)Cl and Pt(N^N^C)Cl, Pt(N^C^N)Cl has the highest emission energy, consistent with above anticipation. The higher emission energy further supports the larger emission efficiency of Pt(N^C^N)Cl, because the nonradiative decay rate from the T_1 decreases exponentially with increasing T_1–S_0 gap, a mechanism known as the energy gap law [38].

Note that no spin-orbit interactions are included within the TD-DFT results presented above. However, it seems to be a more general property of organo-transition metal compounds that the lowest triplet substate represents an almost pure triplet and mix with a little of singlet character.

Table 7 Calculated excitation energies of T_1 and their transition nature for Pt(II) complexes

	Calc. (nm)	Composition	*f*	State	Nature	Exp. (nm)
Pt(N^N^N)Cl	598	L → H (0.71)	0.000	T_1	$d_{Pt}/P_{Cl} \rightarrow \pi^*_L$	
Pt(N^C^N)Cl	533	L → H (0.68)	0.000	T_1	$d_{Pt}/\pi_{phenyl}/P_{Cl} \rightarrow \pi^*_L$	524, 491 [16]
Pt(N^N^C)Cl	738	L → H (0.72)	0.000	T_1	$d_{Pt}/\pi_{phenyl} \rightarrow \pi^*_L$	
Pt-4	510	L → H (0.67)	0.000	T_1	$d_{Pt}/\pi_{phenyl}/P_{Cl} \rightarrow \pi^*_L$	470 [8]
1	500	L → H (0.72)	0.000	T_1	$d_{Pt}/\pi_{phenyl}/P_{Cl} \rightarrow \pi^*_L$	

L cyclometalated ligands

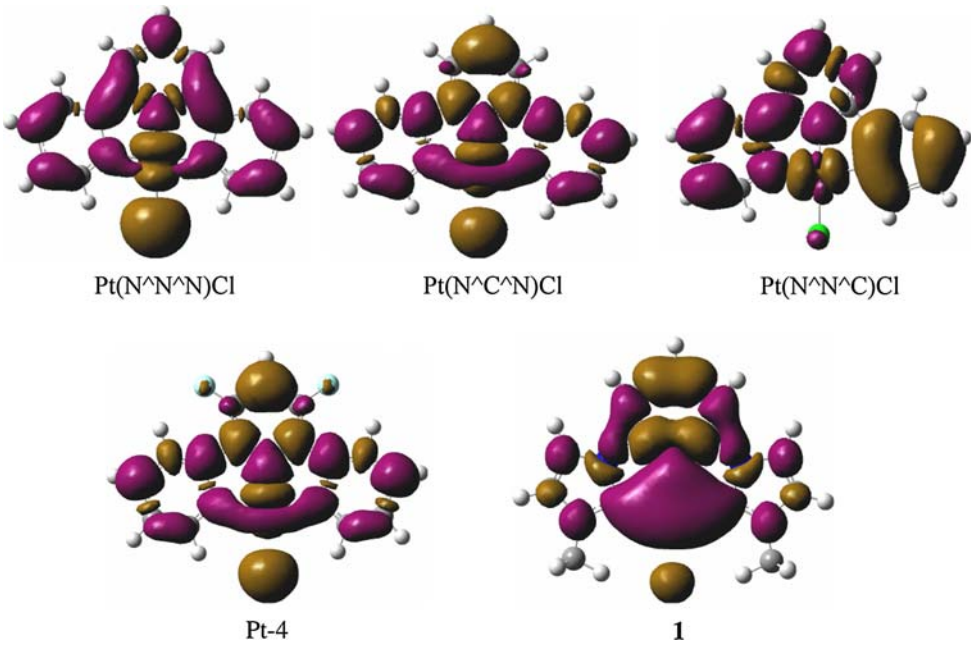

Fig. 3 Change of electron density distribution upon the $T_1 \rightarrow S_0$ electronic transition. *Yellow* and *violet* colors correspond to a decrease and increase of electron density, respectively

This has been observed experimentally for many compounds [39]. Thus, spin-orbit interactions have a little effect on the lowest triplet excited state, and the TD-DFT results presented above are still reliable.

3.5 Design of a new blue emitter

Efficient blue phosphorescent materials are relatively few as compared with the reported efficient green and red ones. Considering the advantages of Pt(N^C^N)Cl which is an efficient cyan emitter [16], we attempt to modify this molecule to design new efficient blue phosphorescent molecules comparable to a blue emitter Pt-4 reported previously [8] (see Fig. 4).

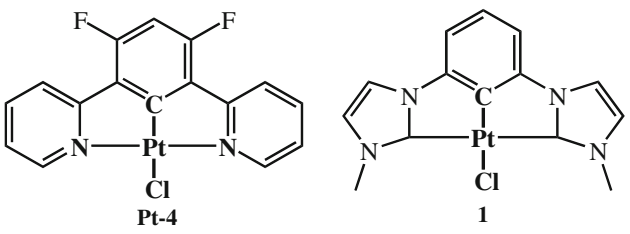

Fig. 4 The structures of the designed molecule **1** and Pt-4

Thompson and his coworkers have synthesized an iridium complex emitting near-UV phosphorescence *via* replacing the pyridine fragments of $Ir(ppy)_3$ (ppy = 2-phenylpyridine) with an *N*-heterocyclic carbene-based group [40], and they also proposed that luminescent compounds with carbene ligands can be employed in OLED [41]. Similarly, this type of group, 3-methylimidazolin-2-ylidene, is also adopted instead of pyridine groups in Pt(N^C^N)Cl. The resulting molecular structure of **1** is shown in Fig. 4.

The energies of the lowest triplet excited states of the designed molecule **1** and Pt-4 are listed in Table 7. A graphical display for the changes of electron density distribution upon $T_1 \rightarrow S_0$ excitation is also shown in Fig. 3. The luminescent characters of **1** and Pt-4 are $d_{Pt}/\pi_{phenyl}/\pi_{A4} \rightarrow \pi^*_L$ (see Fig. 3 and Table 7), similar to Pt(N^C^N)Cl.

Table 8 The difference between the calculated coordination bond length of S_0 and T_1 states for the designed molecule and Pt-4 (unit: Å)

	1	Pt-4
Pt–A_1	−0.053	−0.023
Pt–A_2	−0.002	0.000
Pt–A_3	−0.002	0.000
Pt–A_4	−0.004	−0.026

In general, TD-DFT method systematically underestimates the transition energies, although it reproduces the general trend. For example, the calculated wavelength of Pt-4 (510 nm) is longer than that obtained in experiment (470 nm). The calculated emission wavelength of **1** is 500 nm, close to that of Pt-4. Accordingly, we presume that the designed molecule can be served as a blue emitter.

Furthermore, the excited-state geometry relaxation of **1** and Pt-4 is also evaluated. The difference between the calculated coordination bond length of S_0 and T_1 states for **1** and Pt-4 are tabulated in Table 8. Their change in coordination bond length is small and similar to that of Pt(N^C^N)Cl. The Δr_{e-g} values listed in Table 4 are also employed to evaluate the geometry relaxation on cyclometalated ligands of **1** and Pt-4. Like Pt(N^C^N)Cl, the Δr_{e-g} values of Pt-4 (−0.005 Å) and **1** (−0.007 Å) are very little. It follows that Pt-4 and **1** have small geometry relaxation. Hence, compared with the Pt(N^C^N)Cl and Pt-4, the designed molecule **1** is thought to be a potentially efficient blue emitter from the aspects of nonradiative relaxation and the luminescent character and energy.

Moreover, to rationalize the results, one might consider the radiative rate, which partially depends on the $S_1 \rightarrow T_n$ intersystem crossing (ISC) due to spin-orbit interactions of the triplet states with singlet states. A quantitative analysis of ISC will require the calculation of the singlet/triplet potential surfaces and the spin-orbit coupling (SOC) from S_1 to the triplet is manifold [42]. Here, we qualitatively describe the ISC rate as function of S_1–T_n energy separation [43]. To simplify the approach, we just consider the $S_1 \rightarrow T_1$ and $S_1 \rightarrow T_2$ ISC process.

Figure 5 shows that the calculated relative energy levels obtained in the S_1 excited state conformation. It can be seen that the energies of S_1 for these complexes are significantly higher than that of T_1. Thus, the interaction of S_1 with T_1 is weak and T_1 is a little affected by singlet states, which further demonstrates the reliability of results of the lowest triplet states calculated by the TD-DFT method. Obviously, the $S_1 \rightarrow T_2$ transition is the dominant ISC process. The S_1–T_2 energy separation is 0.48, 0.34, 0.37, 0.38, and 0.00 eV for Pt(N^N^N)Cl, Pt(N^N^C)Cl, Pt(N^C^N)Cl, Pt-4 and **1**, respectively. The ISC rate decreases exponentially as the singlet-triplet gap increases [43]. The S_1–T_2 energy separation of Pt(N^N^C)Cl,

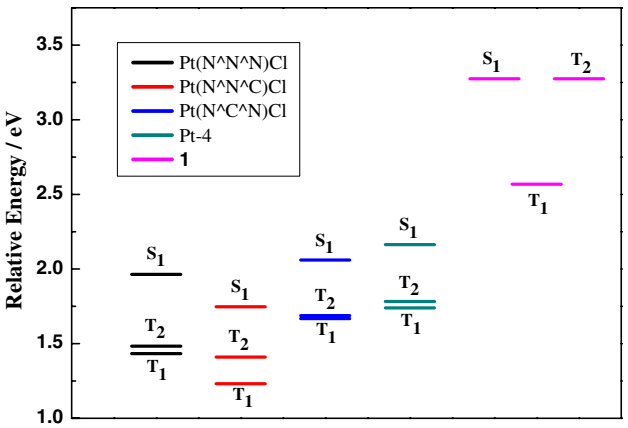

Fig. 5 Calculated relative energy levels in the S_1 excited state conformation

Pt(N^C^N)Cl and Pt-4 are close to each other and smaller than that of Pt(N^N^N)Cl; thus the ISC rates of these three complexes should be nearly the same and larger than that of Pt(N^N^N)Cl. In experiment, the radiative rates of these four complexes are all between 10^4 and 10^5 s^{-1}, and that of Pt(N^N^N)Cl is relatively small [8, 13, 14, 16].

The energy of S_1 of **1** is almost equal to that of T_2, resulting in the larger interaction between these two excited states. It follows that the $S_1 \rightarrow T_2$ ISC is quite fast in the designed molecule **1**. The large ISC rate helps to promote the radiative rate. Therefore, the high emission efficiency of **1** is also supported by the large ISC rate. We hope our observation can be further demonstrated by experiment.

4 Conclusion

Three platinum(II) complexes Pt(N^N^N)Cl (N^N^N = terpyridine), Pt(N^C^N)Cl (N^C^N = 1,3-di(2-pyridyl)-benzene) and Pt(N^N^C)Cl (N^N^C = 6-phenyl-2,2′-bi-pyridines) are selected to study the effect of the presence and position of phenyl group on the electronic and phosphorescent properties by using quantum theoretical calculations. The calculated results show that the presence and position of phenyl group significantly affect the molecular and electronic structures, charge distribution and phosphorescent properties. Due to the strongest feedback from Pt to phenyl group, the coordination bond length trans to phenyl group is the longest among the same type of bonds. The strong σ-donor ability of Pt–C bond makes more electrons center at Pt atom and the fragments trans to phenyl group. In the luminescent process, because the phenyl group participates to the constitution of transition orbitals, the luminescent nature is different for the three molecules. The direction of $\pi_{phenyl} \rightarrow \pi^*_{pyridines}$ charge transfer of Pt(N^N^C)Cl differs from that of Pt(N^C^N)Cl owing to the different position of phenyl group. Moreover,

the presence and position of phenyl group also influence the geometry relaxation between the ground and the lowest triplet states. Compared with Pt(N^N^N)Cl and Pt(N^N^C)Cl, Pt(N^C^N)Cl has the smallest excited-state geometry relaxation and the biggest emission energy and spatial overlap between the transition orbitals in emission process. This leads to the largest emission efficiency of Pt(N^C^N)Cl, which agrees well with the experimental observation. Thus, based on the Pt(N^C^N)Cl, new blue emitters are designed. The complex using 3-methylimidazolin-2-ylidene to instead of pyridine groups in Pt(N^C^N)Cl may be a potentially efficient blue emitting material.

Acknowledgments The authors gratefully acknowledge the financial support from the National Natural Science Foundation of China (Project Nos. 20373009, 20573016 and 20703008), Chang Jiang Scholars Program (2006), Program for Changjiang Scholars and Innovative Research Team in University (IRT0714), the Science Foundation for Young Teachers of NENU (No. 20081002, 20070304 and 20070309), and the Training Fund of NENU's Scientific Innovation Project (NENU-STC07017). The Opening Project of Key Laboratory for Chemistry of Low-Dimensional Materials of Jiangsu Province (No. JSKC07034) is also greatly appreciated.

References

1. Williams JAG, Develay S, Rochester DL, Murphy L (2009) Coord Chem Rev 252:2596–2611
2. Lu W, Mi BX, Chan MCW, Hui Z, Che CM, Zhu N, Lee ST (2004) J Am Chem Soc 126:4958. doi:10.1021/ja0317776
3. Cocchi M, Fattori V, Virgili D, Sabatini S, Di Marco P, Maestri M, Kalinowski J (2004) Appl Phys Lett 84:1052. doi:10.1063/1.1646214
4. Ma B, Djurovich PI, Garon S, Alleyne B, Thompson ME (2006) Adv Funct Mater 16:2438. doi:10.1002/adfm.200600614
5. D'Andrade BW, Brooks J, Adamovich V, Thompson ME, Forrest SR (2002) Adv Mater 14:1032. doi:10.1002/1521-4095(20020805)14:15<1032::AID-ADMA1032>3.0.CO;2-6
6. He Z, Wong WY, Yu X, Kwok HS, Lin Z (2006) Inorg Chem 45:10922. doi:10.1021/ic061566c
7. D'Andrade BW, Forrest SR (2003) J Appl Phys 94:3101. doi:10.1063/1.1597942
8. Yang XH, Wang ZX, Madakuni S, Li J, Jabbour GE (2008) Adv Mater 20:2405. doi:10.1002/adma.200702940
9. Yip HK, Cheng LK, Cheung KK, Che CM (1993) J Chem Soc Daltan Trans 2933
10. Wong KH, Chan MCW, Che CM (1999) Chem Eur J 5:2845. doi:10.1002/(SICI)1521-3765(19991001)5:10<2845::AID-CHEM2845>3.0.CO;2-G
11. Brooks J, Babayan Y, Lamansky S, Djurovich PI, Tsyba I, Bau R, Thompson ME (2002) Inorg Chem 41:3055. doi:10.1021/ic0255508
12. Aldridge TK, Stacy EM, McMillin DR (1994) Inorg Chem 33:722. doi:10.1021/ic00082a017
13. Field JS, Haines RJ, Ledwaba LP, McGuire R Jr, Munro OQ, Low MR, McMillin DR (2007) Daltan Trans 192
14. Lai SW, Chan MCW, Cheung TC, Peng SM, Che CM (1999) Inorg Chem 38:4046. doi:10.1021/ic990238s
15. Mdleleni MM, Bridgewater JS, Watts RJ, Ford PC (1995) Inorg Chem 34:2334. doi:10.1021/ic00113a013
16. Williams JAG, Beeby A, Davies ES, Weinstein JA, Wilson C (2003) Inorg Chem 42:8609. doi:10.1021/ic035083+
17. Koch W, Holthausen MCA (2000) Chemist's guide to density functional theory. Wiley-VCH, Weinheim
18. Adamo C, di Matteo BV (1999) Adv Quantum Chem 36:4
19. Nguyen KA, Kennel J, Pachter R (2002) J Chem Phys 117:7128. doi:10.1063/1.1497640
20. Stoyanov SR, Villegas JM, Rillema DP (2003) Inorg Chem 42:7852. doi:10.1021/ic030084n
21. Becke AD (1993) J Chem Phys 98:5648. doi:10.1063/1.464913
22. Lee C, Yang W, Parr RG (1988) Phys Rev B 37:785. doi:10.1103/PhysRevB.37.785
23. Miehlich B, Savin A, Stoll H, Preuss H (1989) Chem Phys Lett 157:200. doi:10.1016/0009-2614(89)87234-3
24. Casida MK, Jamorski C, Casida KC, Salahub DR (1998) J Chem Phys 108:4439. doi:10.1063/1.475855
25. Stratmann RE, Scuseria GE (1998) J Chem Phys 109:8218. doi:10.1063/1.477483
26. Pyykkö P, Mendizabal F (1998) Inorg Chem 37:3018. doi:10.1021/ic980121o
27. Zhang RQ, Li QS (2008) Theor Chem Acc 119:437. doi:10.1007/s00214-007-0400-9
28. Zhou X, Pan QJ, Xia BH, Li MX, Zhang HX, Tung AC (2007) J Phys Chem A 111:5465. doi:10.1021/jp064044r
29. Zhou X, Zhang HX, Pan QJ, Xia BH, Tung AC (2005) J Phys Chem A 109:8809. doi:10.1021/jp0503359
30. Frisch MJ et al (2004) Gaussian 03, revision C.02. Gaussian, Wallingford
31. Cardenas DJ, Echavarren AM, de Arellano MCR (1999) Organometallics 18:3337. doi:10.1021/om990125g
32. Hofmann A, Dahlenburg L, van Eldik R (2003) Inorg Chem 42:6528. doi:10.1021/ic034400+
33. Liao Y, Shi LL, Feng JK, Yang L, Ren AM (2006) J Theor Comput Chem 5:401. doi:10.1142/S0219633606002349
34. Kan YH, Yang GC, Yang SY, Zhang M, Lan YQ, Su ZM (2006) Chem Phys Lett 418:302. doi:10.1016/j.cplett.2005.11.005
35. Cheung TC, Cheung KK, Peng SM, Che CM (1996) J Chem Soc Daltan Trans 1645
36. Sotoyama W, Satoh T, Sato H, Matsuura A, Sawatari N (2005) J Phys Chem A 109:9760. doi:10.1021/jp053366c
37. Turki M, Daniel C, Zalis S, Vlcek A, van Slageren J, Stufkens DJ (2001) J Am Chem Soc 123:11431. doi:10.1021/ja010782b
38. Wilson JS, Chawdhury N, Al-Mandhary MRA, Younus M, Khan MS, Raithby PR, Kohler A, Friend RH (2001) J Am Chem Soc 123:9412. doi:10.1021/ja010986s
39. Yersin H (ed) (2008) High efficient OLEDs with phosphorescent materials. Wiley-VCH, Weinheim. ISBN: 978-3-527-40594-7
40. Sajoto T, Djurovich PI, Tamayo A, Yousufuddin M, Bau R, Thompson ME (2005) Inorg Chem 44:7992. doi:10.1021/ic051296i
41. Thompson ME, Tamayo A, Djurovich P, Sajoto T, Forrest SR, Mackenzie PB, Walters R, Brooks J, Li X-C, Alleyne B, Tsai J-Y, Lin C, Ma B, Barone MS, Kwong R (2005) Luminescent compounds with carbene ligands. Pub. No.: WO/2005/113704. International Applicatio No. PCT US2005(017336)
42. Kleinschmidt M, Tatchen J, Marian CM (2002) J Comput Chem 23:824. doi:10.1002/jcc.10064
43. Burin AL, Ratner MA (1998) J Chem Phys 109:6092. doi:10.1063/1.477236